



## Dynamics of the mobile insert helix in the domain III–IV of Aux/IAA17 probed by site-directed spin labeling and paramagnetic NMR spectroscopy

Mookyoung Han and Jeong-Yong Suh\*

Department of Agricultural Biotechnology, Seoul National University, 1 Gwanak-ro, Gwanak-gu, Seoul 151-921, Korea

Received Aug 2, 2015; Revised Sep 7, 2015; Accepted Sep 25, 2015

**Abstract** The plant hormone auxin is involved in all stages of plant development. Aux/IAAs are the transcriptional repressors that bind to the Auxin Response Factors (ARFs) to regulate the gene expression upon auxin release. Aux/IAA have highly conserved C-terminal domains (domains III–IV) that mediate both homotypic and heterotypic interactions between Aux/IAA and ARF family proteins. Recent studies revealed that the conserved domains III–IV share a common  $\beta$ -grasp fold that oligomerizes in a front-to-back manner.<sup>1,2,3</sup> In particular, Aux/IAA contains a mobile insert helix in the domain III–IV, whereas ARFs do not. Here, we investigated the dynamics of the insert helix using paramagnetic NMR spectroscopy. The insert helix exhibited fast motions in the ps-ns time scale from <sup>15</sup>N relaxation data, but the amplitude of the motion is likely limited to the local neighborhood. Our result suggests that the motion of the helix may have functional implications in protein–protein interactions for transcriptional regulations.

**Keywords** auxin, Aux/IAA17, NMR, PRE

### Introduction

Auxin is a phyto-hormone that mediates the cell division and elongation for plant growths and developments. Aux/IAA and auxin response factors

(ARFs) regulate the expression of auxin response genes. ARFs consist of four conserved domains: Domain I is an amino-terminal DNA-binding domain that recognize TGTCTC auxin response elements. Following domain I, there is a non-conserved middle region (Domain II) that functions as either a transcriptional activator or a repressor. Domain III and IV are highly conserved in the carboxyl terminus, which forms the scaffold for the hetero-dimerization with Aux/IAA proteins.

Aux/IAA (IAA) proteins are transcriptional repressors and also contain four conserved domains. The amino terminal domain I is the co-repressor binding domain that binds to topless (TPL) protein for transcriptional suppression. Domain II is the 13-residue degron domain for auxin-induced protein degradation. Domain II is recruited to the F-box protein with the auxin between the two proteins, by which Aux/IAA is ubiquitinated and degraded by the 26S proteasome.<sup>1</sup> The carboxyl terminal domains III and IV facilitate homotypic and heterotypic interaction among IAA and ARF family members, which are required for the transcriptional regulation of the auxin-responsive gene expression. These structures of the C-terminal domain III–IV of *Arabidopsis* have been reported for Aux/IAA17, ARF5, and ARF7, which represents a type I/II PB1 fold with both acidic and basic faces, and mediates homotypic and heterotypic interactions in a front-to-back manner.<sup>2</sup>

\* Address correspondence to: **Jeong-Yong Suh**, Department of Agricultural Biotechnology, Seoul National University, 1 Gwanak-ro, Gwanak-Gu, Seoul, 151-921, Korea, Tel: 82-2-880-4879; Fax: 82-2-877-4906; E-mail: jysuh@snu.ac.kr

In *Arabidopsis thaliana*, approximately half of the Aux/IAA family proteins contain a long insert sequence between the domain III and the domain IV, whereas none of the ARF family proteins carries the insert sequence (Figure 1).<sup>1-4</sup> The structures of the domain III–IV are similar between Aux/IAA17 and ARF5 and ARF7, except for the insert region. We previously reported that the dynamic  $\alpha$ I' helix did not participate in the folding nor in the homo- or heterotypic oligomerization,<sup>1</sup> and the function is not yet been discovered. <sup>15</sup>N R<sub>1</sub> and R<sub>2</sub> relaxation rates as well as <sup>1</sup>H–<sup>15</sup>N heteronuclear NOE measurements showed that  $\alpha$ I' helix exhibited fast motions in the picosecond to nanosecond time scale.<sup>1</sup> Here we employed the site-directed spin-labeling and the paramagnetic relaxation enhancements (PRE) to probe the amplitude of the motion of the  $\alpha$ I' helix. Based on the fact that PRE by the nitroxide spin label can be observed at distances up to 27 Å, the motion of the  $\alpha$ I' helix was qualitatively examined. Two positions spin-labeled by MTSL were shown in Figure 2.

## Experimental Methods

**Mutation, Expression and Purification of Aux/IAA17 constructs-** Domain III–IV (G109–L217) of Aux/IAA17 was cloned into a pET28a vector (Merck Millipore) with an N-terminal His<sub>6</sub> tag. Mutations were introduced to generate for spin labeling: Phe148Cys and Phe162Cys mutations were introduced into the D183N/D187N construct (the construct that produced a monomeric protein) for Aux/IAA17. Extra cysteine residues were further mutated into alanine residues to avoid unwanted conjugation reactions, such that the C203A mutation was introduced into the domain III–IV. Site-directed mutagenesis was performed using the Quik-Change Kit (Agilent Technology), and the new constructs were verified by DNA sequencing.

The expression of the Aux/IAA domain was performed using the expression vector pET28a in Codon+ *E. coli* cells. Transformed cells were grown in minimal media (with <sup>15</sup>NH<sub>4</sub>Cl) as the sole nitrogen sources. The cells transformed by the expression



**Figure 1.** Multiple sequence alignment of Aux/IAA in *Arabidopsis*

The *Arabidopsis thaliana* encodes 29 Aux/IAA proteins that contain carboxyl-terminal domain. These carboxyl-terminal domains have conserved Lys (red shade) for the basic face and Asp (blue shade) for the acidic face. The domain III–IV of Aux/IAA17 is similar to that of ARF5, ARF7 and PsIAA4,<sup>1-4</sup> except for the insert  $\alpha$ I' helix between the domains III and IV (red box).

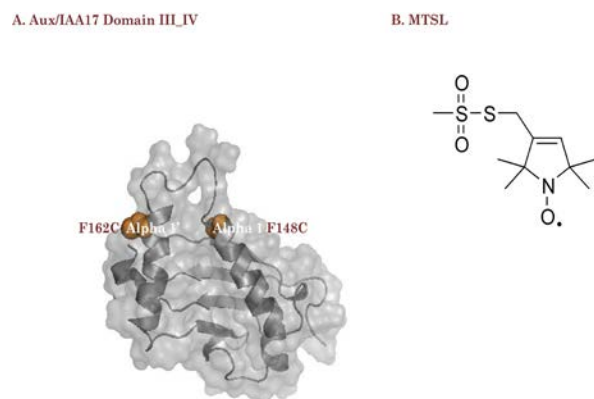


**Figure 2.** Spin label residue on Aux/IAA17 structure  
 A. Front views of the solution structure of Aux/IAA17. The point mutation residues F148C, and F162C for spin labeling are highlighted. B. Structure of MTSL spin label.

vector were cultured at 37°C to an  $OD_{600}$  of 0.8, and protein overexpression was induced by adding isopropyl- $\beta$ -D-thiogalactopyranoside (IPTG) to a final concentration of 1mM, followed by induction for 12h at 18°C. The cells were harvested by centrifugation, and resuspended in buffer [20 mM Tris-HCl (pH 7.4), 200 mM NaCl, 1 mM phenylmethanesulfonyl fluoride (PMSF)], and disrupted by emulsiflex. The lysate was centrifuged to remove insoluble debris. The supernatant was loaded on a His-trep column equilibrated with binding buffer [20mM Tris-HCl (pH7.4), 200mM NaCl] and was eluted with a gradient concentration of Imidazole. The solutions containing protein were separated by a HiLoad Superdex 75 column [20 mM Tris-HCl (pH 7.4), 200 mM NaCl] and finally were purified by Mono Q column. The Aux/IAA and ARFs were analyzed by SDS-PAGE to confirm sample mass and sample purity.

**NMR Experiments-** The NMR HSQC were monitored by recording 2D  $^1\text{H}$ - $^{15}\text{N}$  HSQC spectra at 25°C on a Bruker 900 MHz spectrometer equipped with a cryoprobe.<sup>7</sup> For HSQC characterization, all protein samples were prepared at a concentration of 0.3 mM in 10 mM sodium phosphate, pH 7.4, containing.

NMR spectra were processed using the NMRView programs.

**MTSL nitroxyl radical labelling-** MTSL was conjugated to the Aux/IAA mutants via a disulfide bond with the cysteine residue.

## Results and Discussions

**Spin labeling design based on the structure.-** The Spin label MTSL [1-oxy-2,2,5,5-tetramethylpyrroline-3-methyl]-methane-thiosulfonate] was conjugated to the proteins via surface-engineered cysteine residues. We designed two single-cysteine mutants of Aux/IAA17 for the introduction of the nitroxide spin label MTSL based on the three-dimensional solution structure. One position was in the C-terminus of the  $\alpha\text{I}$  helix (F148C), and the other was in the beginning of the  $\alpha\text{I}'$  helix (F162C) as shown in Figure2. These positions were designed to cover a sufficient space near the  $\alpha\text{I}'$  helix to determine whether the  $\alpha\text{I}'$  helix fluctuate widely and reach distant areas.

**Paramagnetic effect from MTSL spin-labeled constructs-** To get the information on the motion of the  $\alpha\text{I}'$  helix in the Aux/IAA17 domain III-IV, we measured the paramagnetic line broadening. The NMR samples used for the PRE measurement comprised 0.3 mM  $^1\text{H}/^{15}\text{N}$ -labeled Aux/IAA17 mutants. Increase of the transverse relaxation rates of the backbone amide groups resulted in the reduction of the signal intensity of the affected nuclei. The line width of the proton and nitrogen resonances would be significantly broadened when the amide groups were placed within 27.0 Å of the paramagnetic MTSL spin label, and fully broadened out if the distances were less than 10.5 Å due to its fast transverse relaxation rate<sup>5</sup>.

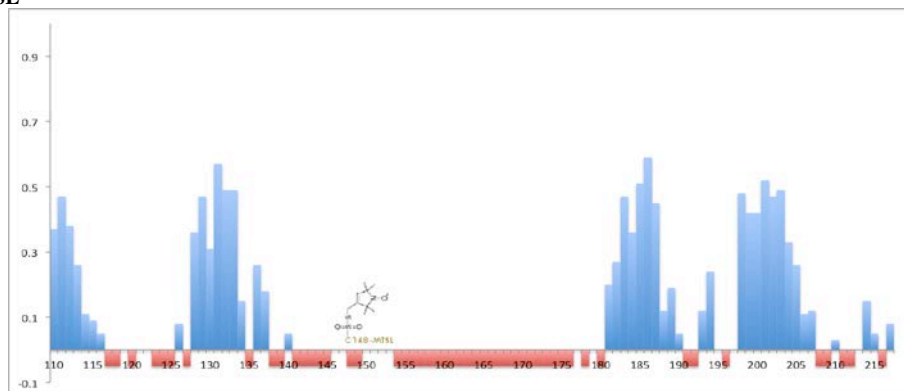
We performed 2D  $^1\text{H}$ - $^{15}\text{N}$  heteronuclear single quantum correlation (HSQC) spectra of each Aux/IAA17 spin-labeled paramagnetic samples and the diamagnetic samples. Differential line

broadenings were observed according to the PRE, and the intensity ratio between the paramagnetic and diamagnetic samples were obtained for individual amide groups using the  $^1\text{H}$ - $^{15}\text{N}$  HSQC spectrum. Changes in HSQC cross-peak intensities of the spin-labeled Aux/IAA mutants (I) in comparison to diamagnetic Aux/IAA mutants ( $I_0$ ) were plotted in a bar graph, as shown in Figure 3. The bar graph indicates that most of the residues that showed decreases in cross-peak intensity ( $I/I_0 < 0.6$ ), since the domain III–IV of Aux/IAA17 is a small-size protein with the length of the longest dimension as 20 Å. Many amide groups before and after the spin-labeling position were completely disappeared due to a large paramagnetic relaxation enhancement

(Figure 3). Amide group resonances that were spatially close to the spin-label were also broadened out beyond detection. On the other hand, amide group resonances that were distal to the spin-label position were broadened to a varying degree according to their distances from the spin-label.

In particular, the F162C spin-labeled sample exhibited localized PREs near the nitroxyl group (Figure 3B). This indicates that the motion of the  $\alpha'$  helix is restricted to the vicinity of the secondary structural element determined in the solution structure. This is illustrated in the three-dimensional structure color-coded by the PRE (Figure 4). The line broadening in F162C-MTSL shows that the PREs prevail near the  $\alpha'$  and  $\alpha\text{I}$  helices. Thus, the  $\alpha'$

#### A. C148-MTSL



#### B. C162-MTSL

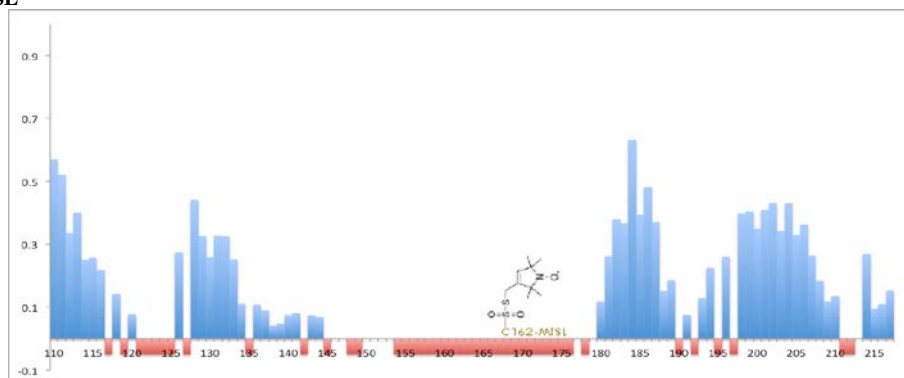


**Figure 3.** Paramagnetic effect from F148C-MTSL and F162C-MTSL.

F148C-MTSL, F162C-MTSL were analyze via the intensity ratio of the amide group cross-peaks. Blank spaces in the diagrams were due to 4 proline residues or unassigned residues. Completely broadened out signals were highlighted in red bar under the axis. A. The spin-labeled side chain Aux/IAA17 (F148C). B. The spin-labeled side chain Aux/IAA17 (F162C).

helix is dynamic in the fast time scale motion, but the amplitude of the motion is not likely large.

The tertiary structures of C-terminal domain III–IV of *Arabidopsis* Aux/IAA17 revealed canonical type I/II PB1 features, which mediated electrostatic front-to-back interaction between protomers via oppositely charged and located surface patches.<sup>1</sup> The Aux/IAA17 contains the longest insert sequence with more than 15 extra residues compared to other ARF family proteins. The insert region forms a helix that

may be in equilibrium between a helix and a coil. Our results demonstrate that the conformational transition is limited to its close local vicinity. It is not clear how the mobility of the insert helix is implicated to the protein–protein interaction and thereby its transcriptional regulation. The role of the dynamics in the  $\alpha I'$  helix will require further characterization of the time scale of the motion using relaxation dispersion.

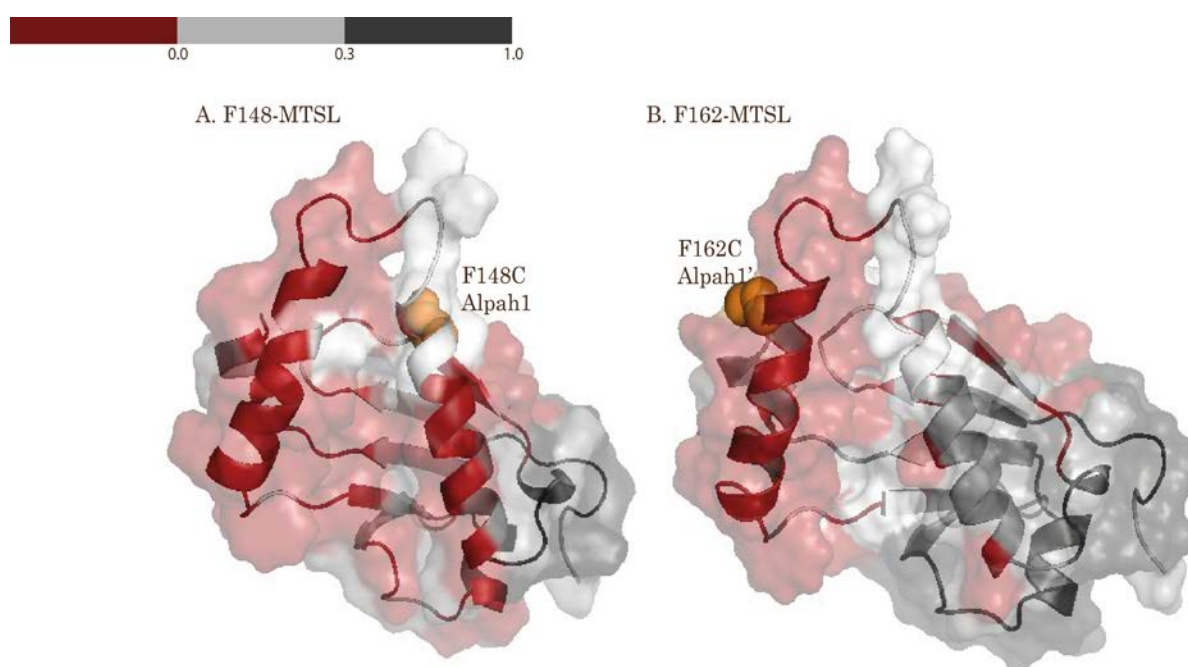


**Figure 4.** Backbone amides with paramagnetic effects in the three-dimensional structure.

A. F148C-MTSL ( $\alpha 1$ ) spin labeling, B. F162C-MTSL ( $\alpha 1'$ ) spin labeling. Results are shown on the ribbon diagram and the transparent surface of the previously determined NMR structure of Aux/IAA17 domain III–IV. The position of the spin-label residue is shown in orange and annotated. Amides that are broadened to undetectable levels are shown in red. Amides that are broadened with measurable intensity ratios  $> 0.3$  are shown in dark gray. White colored residues are either prolines or unassigned signals in  $^{15}\text{N}$ -HSQC spectra.

## Acknowledgements

This study was supported by Research Resettlement Fund for the new faculty of Seoul National University. We thank the high field NMR facility at the Korea Basic Science Institute and the National Center for Inter-

university Research Facilities.

## References

1. M. Han, Y. Park, I. Kim, E. H. Kim, T. K. Yu, S. Rhee, and J. Y. Suh, *Proc. Natl. Acad. Sci. USA*, **111**, 18613 (2014)
2. H. M. Nanao, T. Vinos-Poyo, G. Brunoud, E. Thévenon, M. Mazzoleni, Mast, and R. Dumas, *Nat. commun.*, **5** (2014)
3. D. A. Korasick, C. S. Westfall, S. G. Lee, Nanao, H. M, R. Dumas, G. Hagen, and L. C. Strader, *Proc. Natl. Acad. Sci. USA*, **111**, 5427 (2014)
4. D. C. Dinesh, M. Kovermann, M. Gopalswamy, A. Hellmuth, L. I. A. C. Villalobos, and H. Lilie, S. Abel, *Proc. Natl. Acad. Sci. USA*, **112**, 6230(2015)
5. T. Zheng, A. Boyle, H. R. Marsden, D. Valdink, G. Martelli, and J. Raap, A. Kros, *Org. Biomol. Chem.*, **13**, 1159 (2015)
6. J. Y. Suh, T. K. Yu, Y. J. Yun, and K. O. Lee, *J. Kor. Magn. Reson. Soc.* **18**, 1 (2014)
7. I. G. Lee, K. Y. Lee, J. H. Kim, S. Chae, and B. J. Lee, *J. Kor. Magn. Reson. Soc.*, **17**, 54 (2013)